Article

Not peer-reviewed version

Fungicidal Activity of Secondary Metabolites from *Trichoderma hamatum B-3*

Li Huang , Meng-Dan Liu , Qiang Bian * , Yi-Wen Hu , Li-Juan Chen , Yu-Cheng Gu , Qi-Wei Zu , Guang-Zhi Wang * , Da-Le Guo *

Posted Date: 27 September 2024

doi: 10.20944/preprints202409.2156.v1

Keywords: Trichoderma; diterpene; sesquiterpene; fungicidal activity

Article

Fungicidal Activity of Secondary Metabolites from *Trichoderma hamatum* b-3

Li Huang [1], Meng-Dan Liu [1], Qiang Bian [2,*], Yi-Wen Hu [1], Li-Juan Chen [1], Yu-Cheng Gu [3], Qi-Wei Zu [4], Guang-Zhi Wang [1,*] and Da-Le Guo [1,*]

[1] State Key Laboratory of Southwestern Chinese Medicine Resource, School of Pharmacy, Chengdu University of Traditional Chinese Medicine, Chengdu, 611137 China (G.-Z.Wang; D.-L. Guo)
[2] National Pesticide Engineering Research Center (Tianjin), College of Chemistry, Nankai University, Tianjin, 300071, China (Q. Bian)
[3] Syngenta Jealott's Hill International Research Centre, Syngenta, Berkshire, RG42 6EY, UK
[4] Department of biochemistry, College of art&science, Baylor University, Texas 76706, USA
* Correspondence: bianqiangnankai.edu.cn (Q. Bian); wangguangzhi@cdutcm.edu.cn (G.-Z.Wang); guodale@cdutcm.edu.cn (D.-L. Guo)

Abstract: Two new harziane diterpenes (**1-2**), five undescribed cyclonerane sesquiterpenes (**3-7**) and three known compounds, 11-cycloneren-3,7,10-triol (**8**), harziandione (**9**), and dehydroacetic acid (**10**) were isolated from *Trichoderma hamatum* b-3. Their structures were elucidated via comprehensive inspection of spectral evidences in HRESIMS, 1D and 2D NMR, the absolute configuration of **1-8** was confirmed by NMR, ECD calculation as well as Mosher's method. *In vitro* fungicidal activity showed that some compounds showed great inhibitory activity against pathogenic fungi including *Fusarium graminearum*, *Sclerotinia sclerotiorum*, *Botrytis cinerea*, *and Rhizoctonia solani*, among which compound **10** showed 100% inhibition of *S. sclerotiorum* and *B. cinerea*. *In vivo* activity test showed that compound **10** was 65.8% effective against *B. cinerea* and has the potential to be developed as a biocontrol pesticide.

Keywords: *Trichoderma*; diterpene; sesquiterpene; fungicidal activity

1. Introduction

The continuous growth of the global population exerts tremendous pressure on agricultural production systems. Concurrently, the food and economic losses caused by plant pathogens in agriculture have raised serious concerns [1,2]. Chemical control can mitigate plant diseases and enhance grain yield, making it one of the most effective methods for prevention and control. However, the frequent use of chemical pesticides can result in pesticide residues in crops; contaminate soil and water sources; as well as pose risks to human health [3,4]. In contrast, biological control involves managing plant diseases through microorganisms and their metabolites, offering a safer, more effective, and environmentally friendly alternative to chemical control [5]. *Trichoderma* strains are widely utilized in the biological control of plant diseases within agriculture, employing diverse mechanisms such as competition, antibiosis, induced systemic resistance and mycoparasitism [6–9].

Antibiosis is a primary biological control mechanism employed by *Trichoderma*, which involves the production of secondary metabolites that inhibit the growth of pathogenic fungi [10,11]. *Trichoderma* strains are known to produce a diverse array of natural products, including epipolythiodioxopiperazines [12], peptaibols [13], pyrones [14], butenolides [15], koninginins [16], steroids [17], lactones [18], and trichothecenes [19,20]. Our research team has been dedicated to the study of fungal secondary metabolites with bioactive properties over an extend period, resulting in the isolation of several previously undescribed compounds from fungal strains such as *Chaetomium elatum* [21], and *Nigrospora sphaerica* [22]. In this study, we investigated the secondary metabolites of *Trichoderma hamatum*, leading to the isolation of two new harziane diterpenes (**1-2**) and five cyclonerane sesquiterpenes (**3-7**). The structures of these compounds were determined by HRESIMS, NMR, ECD, Mosher's method [23] combined with chemical calculation. Compounds **1-10** were tested

 doi:10.20944/preprints202409.2156.v1

for their in vitro fungicidal activity against six agriculture pathogenic fungi. Compound **10** was then tested for in vivo fungicidal activities against some pathogenic fungi. Herein, we report the details of isolation, elucidation and fungicidal activity of above-mentioned secondary metabolites.

2. Materials and Methods

2.1. General Experimental Procedures

Optical rotation was measured on a Perkin-Elmer 241 Polarimeter (Perkin Elmer, Inc., Waltham, MA, USA). UV, CD and ICD spectra were measured on a Chirascan circular dichroism (Applied Photophysics Ltd., Leatherhead, UK). IR spectrum was acquired from an Agilent Cary 600 FT-IR infrared spectrometer (Agilent Technologies, Santa Clara, USA). Mass spectrum was obtained on an Ultra-performance liquid chromatography coupled with Q Exactive Quadrupole-Electrostatic field Orbital trap high resolution mass spectrometer (Thermo Fisher Scientific, Bremen, Germany). NMR spectra were measured with a Bruker Ascend 600 MHz (Burker, Karlsruhe, Germany) with TMS as internal standard. Fractionation was conducted on a Column chromatography silica gel (200-300 mesh). Sample fractionated by dynamic axial compression column (Hanbon Sci.& Tech, Huaian, China). Purification was performed with a NP7000 preparative high performance liquid chromatograph (Hanbon Sci.& Tech, Huaian, China) with a kromasil C18 5 μm semi-preparative column (10×250 mm). Methanol, acetone, ethyl acetate are analytical pure and dimethyl sulfoxide (chromatographic pure) were purchased from Chengdu Kelong Chemical Co., Ltd. Dichloromethane (analytically pure), methanol (chromatography preparative pure) and acetonitrile (chromatography preparative pure) were purchased from Chengdu Jinshan Chemical Reagent Co., Ltd. Deuterated chloroform was purchased from Adamas Reagent Co., Ltd. N, N-dimethylformamide (analytically pure) was purchased from Tianjin Fuyu Fine Chemical Co. Ltd. Pyrimethanil and dimethachlon (analytically pure) were purchased from Alta Scientific Co., Ltd.

2.2. Fungal Material and Fermentation

The strain (GenBank accession no. OR553890, sequence no. NR134371.1) was isolated from the rhizomes of *Bergenia purpurascens* collected from Mount Emei and identified to be *T. hamatum* by Shanghai Sangong Bioengineering Co., Ltd. through morphological analysis and BLAST comparison.

Fungus 2 medium (maltose 20 g; monosodium glutamate 10 g; dextrose 10 g; yeast paste 3 g; corn syrup 1 g; mannitol 20 g; KH_2PO_4 0.5 g; $MgSO_4.7H_2O$ 0.3 g; $CaCO_3$ 20 g; 5-azacytidine 10 mg; distilled water 1 L) was used for the cultivation of *T. hamatum* b-3[24]. The experimental strains were inoculated onto potato dextrose agar (PDA) medium for duration of 5 days. Subsequently, five pieces (0.5×0.5 cm^2) of mycelial agar plugs were transferred into sterilized and cooled Fungi No. 2 liquid medium contained in 500 mL conical flasks, with 200 mL medium per flask. These flasks were then placed in a constant temperature shaker set at 28 ℃ and 120 rpm/min for 7 days to obtain the *T. hamatum* seed cultures. Following this, the seed cultures were inoculated into the sterilized Fungus 2 medium for expansion cultures, with 2.5 mL of seed cultures added into each 100 mL of medium. The inoculated medium was cultured in a constant temperature shaker at 28 ℃ and 120 rpm/min for 14 days to produce the fermentation broth of *T. hamatum* b-3 resulting in a total culture volume of 564.4 L.

2.3. Extraction and Isolation

The cultured fermentation broth was centrifuged at 4000 r/min in a high-speed centrifuge to separate the fermentation broth. The broth was then treated with an equal volumn of ethyl acetate for 24 h. Subsequently, the extraction process was repeated three times using an equal volume of ethyl acetate. The ethyl acetate layer was collected and concentrated under reduced pressure, yielding 126 g of ethyl acetate extract.

The ethyl acetate extract was separated by silica gel CC, eluted with petroleum ether and acetone (30: 1~1: 1, V/V), yield seven fractions (Fr.1~Fr.7). Fr.1 was separated through column chromatography on dynamic axial compression column (MeOH/H_2O, 90: 10) and semi-pHPLC (MeOH/H_2O, 68: 32) to obtain **9** (11.5, t_R 20.3 min). Fr.2 was separated via RP-18 CC (MeOH/H_2O, 95:5) to afford three fractions (Fr.2.1~ Fr.2.3). Fr.2.1 was then separated through semi-pHPLC (MeOH/H_2O, 50: 50 to 100:0) to obtain eleven fractions (Fr.2.1.1~ Fr.2.1.11), Fr.2.1.5 was then separated through

 doi:10.20944/preprints202409.2156.v1

semi-pHPLC (MeOH/H_2O, 40: 60) to yield **10** (87 mg, t_R 25.8 min). Fr.2.1.6 was subjected to silica gel CC and semi-pHPLC (MeOH/H_2O, 70: 30) to yield **1** (1.8 mg, t_R 28.0 min). Fr.2.1.8 was separated via Sephadex LH-20 CC (CH_2Cl_2/MeOH, 70: 30) and purified by semi-pHPLC (MeCN/H_2O, 20: 80) to produce **8** (13.5 mg, t_R 30.3 min) and semi-pHPLC (MeCN/H_2O, 24: 76) to produce **4** (1.8 mg, t_R 19.7 min) and **5** (9.3 mg, t_R 26.6 min). Fr.3 was separated through dynamic axial compression column chromatography (MeOH/H_2O, 50:50 to 50:100) to give six fractions (Fr.3.1~ Fr.3.6), Fr.3.4 was further purified by CC on Sephadex LH-20 (MeOH) as well as semi-pHPLC (MeCN/H_2O, 57:43) to afford **3** (1.3 mg, t_R 8.3 min). Fr.3.4.1.10 was further purified by semi-pHPLC (MeCN/H_2O, 35: 65) to obtained **6** (1.4 mg, t_R 35.4 min). Fr.5 was separated via dynamic axial compression column chromatography (MeOH/H_2O, 60: 40 to 100: 0) to give five fractions (Fr.5.1~ Fr.5.5), Fr.5.2 was then purified by CC on Sephadex LH-20 (CH_2Cl_2/MeOH, 70:30) and semi-pHPLC (MeCN/H_2O, 40:60) to yield **7** (5.7 mg, t_R 19.4 min).

Compound **1**: Colorless oil; $[\alpha]_D^{20}$ = +81.8 (c = 0.011, MeOH); UV (MeOH) λ_{max} 248 (0.58); IR (KBr): 3449, 2920, 2851, 1740, 1384, 1234, 1026 cm^{-1}; CD (c 2.23 mM, MeOH) λ_{max} ($\Delta\varepsilon$) 238 (-1.21), 295 (0.53), 342 (0.67) nm; HRESIMS m/z 359.2212 $[M+H]^+$ (calcd. For $C_{22}H_{31}O_4^+$, 359.2217); For ^{1}H-NMR, ^{13}C-NMR data see Tables 1 and 2.

Table 1. NMR data for compound **1-2, 6-7** (600 MHz, $CDCl_3$).

pos	**1**	**2**	**6**	**7**
	δ_C, type	δ_C, type	δ_C, type	δ_C, type
1	49.7, C	45.8, C	14.7, CH_3	14.7, CH_3
2	59.4, CH	49.6, CH	44.4, CH	44.4, CH
3	214.2, C	74.4, CH	81.4, C	81.5, C
4	42.7, CH_2	34.3, CH_2	40.5, CH_2	40.5, CH_2
5	30.1, CH	28.2, CH	24.5, CH_2	24.5, CH_2
6	51.8, C	50.4, C	54.6, CH	54.4, CH
7	30.3, CH_2	30.4, CH_2	74.8, C	74.9, C
8	23.8, CH_2	24.6, CH_2	40.5, CH_2	40.0, CH_2
9	141.1, C	154.0, C	22.5, CH_2	22.5, CH_2
10	153.0, C	148.9, C	131.2, CH	129.9, CH
11	196.5, C	200.2, C	129.9, C	130.2, C
12	60.2, CH_2	58.7, CH_2	63.6, CH_2	70.6, CH_2
13	40.4, C	40.4, C	172.4, C	172.3, C
14	52.9, CH	51.4, CH	29.1, CH_2	29.1, CH_2
15	26.7, CH_2	27.6, CH_2	29.3, CH_2	29.3, CH_2
16	25.2, CH_3	26.8, CH_3	172.9, C	172.9, C
17	23.4, CH_3	23.6, CH_3	52.0, CH_3	52.0, CH_3
18	21.1, CH_3	21.4, CH_3	26.2, CH_3	26.2, CH_3
19	20.6, CH_3	21.6, CH_3	25.0, CH_3	25.1, CH_3
20	63.3, CH_2	67.3, CH_2	21.6, CH_3	21.6, CH_3
21	170.9, C			
22	21.0, CH_3			

Table 2. ^{1}H NMR data for compound **1-2, 6-7** (150 MHz, $CDCl_3$).

pos	**1**	**2**	**6**	**7**
	δ_H (J in Hz)	δ_H (J in Hz)	δ_H (J in Hz)	δ_H (J in Hz)
1			1.04, d (6.8)	1.05, d (6.8)

 doi:10.20944/preprints202409.2156.v1

2	2.29, m	1.84, dd (8.2, 3.7)	1.60, m	1.61, m
3		3.98, dd (3.6, 6.6)		
4a	2.90, m	2.42, d (16.9)	1.68, m	1.69, m, 1H
4b	2.09, m	1.50, d (15.3)	1.56, m	1.57, m
5a	2.90, m	2.45, m	1.85, m	1.86, m
5b			1.55, m	1.55, m
6			1.84, m	1.85, m
7a	1.97, m	1.97, m		
7b	1.40, m	1.25, m		
8a	2.29, m	2.40, m	1.49, m	1.51, t (8.4)
8b		2.00, m		
9a			2.19, m	2.12, m
9b			2.12, m	
10			5.41, t (6.7)	5.47, td (7.2, 1.4)
12a	2.66, d (16.6)	2.57, d (16.7)	4.66, d (11.9)	4.48, s
12b	2.51, d (16.4)	2.46, d (16.9)	4.60, d (11.9)	
14	2.52, m	2.14, dd (11.3, 8.9)	2.64, m	2.65, m
15a	2.05, m	1.90, m	2.64, m	2.65, m
15b	1.54, m	1.09, dd (14.0, 9.3)		
16	1.00, s	0.87, s		
17	1.01, s	1.33, s	3.69, s	3.69, s
18	1.13, d (7.2)	1.18, d (7.6)	1.26, s	1.26, s
19	1.54, s	1.51, s	1.15, s	1.17, s
20a	5.12, d (12.8)	4.40, d (18)	1.74, d (1.5)	1.66, d (1.5)
20b	4.76, d (12.9)	4.20, d (18.2)		
22	2.10, s			

Compound **2**: Colorless oil; $[\alpha]_D^{20}$ = +7.1 (*c* = 0.028, MeOH); UV (MeOH) λ_{max} 255 (0.48); IR (KBr): 3439, 2936, 1730, 1643, 1386, 1199 cm^{-1}; CD (c 2.51 mM, MeOH) λ_{max} ($\Delta\varepsilon$) 222 (-0.31), 251 (-0.73), 299 (0.11), 343 (0.53) nm; HRESIMS *m/z* 319.2268 $[M+H]^+$ (calcd. For $C_{20}H_{31}O_3^+$, 319.2268); For ^{1}H-NMR, ^{13}C-NMR data see Tables 1 and 2.

Compound **3**: Colorless oil; $[\alpha]_D^{20}$ = -8.0 (*c* = 0.025, MeOH); UV (MeOH) λ_{max} 209 (4.32); IR (KBr): 3436, 2958, 2926, 2850, 1666, 1622, 1386 cm^{-1}; CD (c 3.05 mM, MeOH) λ_{max} ($\Delta\varepsilon$) 224 (0.33), 321 (-0.12) nm; HRESIMS *m/z* 263.1624 $[M+Na]^+$ (calcd. For $C_{14}H_{24}NaO_3^+$, 263.1618); For ^{1}H-NMR, ^{13}C-NMR data see Tables 3 and 4.

Table 3. NMR data for compound **3-5** and **8** (600 MHz, $CDCl_3$).

pos	**3**	**4**	**5**	**8**
	δ_C, type	δ_C, type	δ_C, type	δ_C, type
1	14.6, CH_3	14.7, CH_3	14.5, CH_3	14.6, CH_3
2	44.6, CH	44.5, CH	44.6, CH	44.5, CH
3	81.4, C	81.5, C	81.6, C	81.4, C
4	40.4, CH_2	40.5, CH_2	40.4, CH_2	40.5, CH_2
5	24.6, CH_2	24.5, CH_2	24.5, CH_2	24.5, CH_2
6	54.9, CH	54.8, CH	54.4, CH	54.8, CH

 doi:10.20944/preprints202409.2156.v1

7	75.0, C	74.7, C	74.8, C	74.8, C
8	43.8, CH_2	36.6, CH_2	43.6, CH_2	35.8, CH_2
9	144.1, CH	29.4, CH_2	126.7, CH_2	29.1, CH_2
10	134.2, CH	76.7, CH	138.1, CH	76.0, CH
11	198.5, C	147.7, C	82.0, C	147.7, C
12	27.2, CH_3	111.2, CH_2	24.6, CH_3	111.0, CH_2
13	26.2, CH_3	26.2, CH_3	26.1, CH_3	26.2, CH_3
14	25.9, CH_3	25.2, CH_3	25.2, CH_3	25.2, CH_3
15		17.8, CH_3	24.2, CH_3	18.2, CH_3

Table 4. ^{1}H NMR data for compound **3-5** and **8** (150 MHz, $CDCl_3$).

pos	**3**	**4**	**5**	**8**
	δ_H (J in Hz)	δ_H (J in Hz)	δ_H (J in Hz)	δ_H (J in Hz)
1	1.06, d (6.8)	1.05, d (= 6.7)	1.04, d (6.7)	1.04, d (6.9)
2	1.62, m	1.62, m	1.60, m	1.59, m
4a	1.72, m	1.69, m	1.68, m	1.69, m
4b	1.58, m	1.57, m	1.56, m	1.57, m
5a	1.91, m	1.86, m	1.86, m	1.87, m
5b	1.58, m	1.56, m	1.57, m	1.56, m
6	1.86, m	1.86, m	1.86, m	1.87, m
8a	2.45, dd (14.8, 7.6)	1.60, m	2.23, m	1.57, m
8b	2.36, dd (13.9, 8.2)	1.48, m		1.50, m
9a	6.88, m	1.65, m	5.74, dt (15.0, 7.4)	1.71, m
9b				1.61, m
10	6.13, d (16.0)	4.05, dd (7.2, 5.3)	5.63, d (15.8)	4.09, dd (7.6, 4.6)
12a	2.27, s	4.95, s	1.32, s	4.97, s
12b		4.84, s		4.86, s
13	1.27, s	1.26, s	1.25, s	1.26, s
14	1.19, s	1.16, s	1.14, s	1.16, s
15		1.74, s	1.33, s	1.72, s

Compound **4**: Colorless oil; $[\alpha]_D^{20}$ = -24.0 (c = 0.05, MeOH); IR (KBr): 3424, 2962, 2875, 1716, 1647, 1455, 1377, 918 cm^{-1}; HRESIMS m/z 279.1940 $[M+Na]^+$ (calcd. For $C_{15}H_{28}NaO_3^+$, 279.1931); For ^{1}H-NMR, ^{13}C-NMR data see Tables 3 and 4.

Compound **5**: Colorless oil; $[\alpha]_D^{20}$ -19.7 (c 0.20, MeOH); UV (MeOH) λ_{max} 213 (0.49); IR (KBr): 3402, 2966, 2931, 1458, 1377, 1156, 920 cm^{-1}; CD (c 2.94 mM, MeOH) λ_{max} ($\Delta\varepsilon$) 216 (-0.05) nm; HRESIMS m/z 271.1910$[M-H]^-$ (calcd. For $C_{15}H_{27}O_4^-$, 271.1914); For ^{1}H-NMR, ^{13}C-NMR data see Tables 3 and 4.

Compound **6**: colorless oil; $[\alpha]_D^{20}$ = -3.2 (c = 0.06, MeOH); IR (KBr): 3453, 2964, 2937, 1737, 1459, 1383, 1211, 1169 cm^{-1}; CD (c 1.62 mM, MeOH) λ_{max} ($\Delta\varepsilon$) 205 (-0.21), 243 (-0.04), 307 (0.3) nm; HRESIMS m/z 393.2249 $[M+Na]^+$ (calcd. For $C_{20}H_{34}NaO_6^+$, 393.2248); For ^{1}H-NMR, ^{13}C-NMR data see Tables 1 and 2.

Compound **7**: Colorless oil; $[\alpha]_D^{20}$ = -4.9 (c = 0.14, MeOH); IR(KBr): 3456, 2968, 2936, 1738, 1438, 1379, 1217, 1163 cm^{-1}; CD (c 2.16 mM, MeOH) λ_{max} ($\Delta\varepsilon$) 221 (0.05) nm; HRESIMS m/z 393.2252 $[M+Na]^+$ (calcd. For $C_{20}H_{34}NaO_6^+$, 393.2248); For ^{1}H-NMR, ^{13}C-NMR data see Tables 1 and 2.

Compound **8**: Colorless oil; $[\alpha]_D^{20}$ = -26.8 (c = 0.28, MeOH); IR (KBr): 3408, 2960, 2873, 1719, 1647, 1455, 1372, 921 cm^{-1}; HRESIMS m/z 279.1941 $[M+Na]^+$ (calcd. For $C_{15}H_{28}NaO_3^+$, 279.1931); For ^{1}H-NMR, ^{13}C-NMR data see Tables 3 and 4.

 doi:10.20944/preprints202409.2156.v1

2.4. NMR and ECD Calculation Methods

The chemical calculations of compounds were conducted using Gaussian 16 [1]. Initially, a conformational analysis was performed with Conflex 8 to generate conformations via Boltzmann Jump [25]. All geometric configurations with relative energies between 0 and 5.0 kcal/mol were optimized at the B3LYP/6-31G level in the gas phase, as well as at ωB97XD/DGDZVP level in methanol. Room-temperature equilibrium populations were determined based on the Boltzmann distribution law [26]. Shielding tensor calculations were conducted at the PCM/mPW1PW91/6-31+G (d, p) level (with Boltzmann distribution ≥1%) employing the GIAO method [27]. The isotropic values of TMS were calculated at the same level and used as a reference. The DP4+ parameters were computed using the Excel file provided by Sarotti [28]. ECD calculations were performed using TD-DFT at the CAM-B3LYP/DGDZVP level in methanol. The ECD spectra were generated by considering the Boltzmann distribution of each geometric conformation. Subsequently, SpecDis 1.71 was utilized to combine the individual CD spectra with a Boltzmann statistical weighting, resulting in a Gaussian curve (σ = 0.16-0.4 eV), which was then compared with experimental data.

2.5. Fungicidal Activity Assay of Compounds 1-10 In Vitro

Pathogenic fungi, including *Alternaria solani*, *Fusarium graminearum*, *Phytophthora capsici*, *Sclerotinia sclerotiorum*, *Botrytis cinerea*, and *Rhizoctonia solani*, were inoculated onto petri dishes containing a compound solution at a concentration of 50 μg/mL. The dishes were then incubated in a biochemical incubator at 25 °C in the dark. The assessment of bactericidal activity was conducted following a three days incubation period, with each experimental group replicated three times. The control group was treated with sterile water. The results of the activity assessment were quantified on a percentage scale ranging from 0 to 100, where 0 indicates no activity and 100 signifies complete eradication [29].

$$\text{Control effect}(\%) = \frac{\text{blank colony diameter} - \text{colony diameter after liquid treatment}}{\text{blank colony diameter} - 4} \times 100$$

2.6. Fungicidal Activity Assay of Compound 10 In Vivo

The commercial fungicides pyrimethanil and dimethachlon were utilized as positive controls in this study. Both compounds, along with the controls, were dissolved in N, N-dimethylformamide and subsequently diluted to a concentration of 200 μg/mL. Cucumber plants were then sprayed with these solutions and allowed to air dry for approximately 2 h. Following this drying period, the undersurfaces of the treated cucumber leaves were sprayed with a pathogen spore suspension containing approximately 1×10^4 spores/mL. The plants were then placed in an incubator maintained at 20 °C with humidity levels exceeding 90% for a 5 day infection period. After this initial incubation, the plants were transferred to a greenhouse for an additional 5 days before being assessed for disease control scores [29].

3. Results

3.1. Structural Identification of Compounds

Compound **1** was isolated as a colorless oil, with its molecular formula determined to be $C_{22}H_{30}O_4$ by HRESIMS, revealing eight degrees of unsaturation. The FT-IR absorption bands indicate the presence of hydroxyl (3449 cm^{-1}), methyl (2920 and 2851 cm^{-1}), carbonyl (1740 cm^{-1}) groups. The ^{1}H-NMR, ^{13}C-NMR (Tables 1 and 2) and HSQC spectra reveal the presence of three carbonyl groups [δ_C: 214.2 (C-3), 196.5 (C-11), 170.9 (C-21)], a set of conjugated double bonds [δ_C: 153.0 (C-10), 141.1 (C-9)], six aliphatic methylene groups [δ_H: 5.12 (H-20a), 4.76 (H-20b), 2.90 (H-4a), 2.66 (H-12a), 2.51 (H-12b), 2.29 (H-8), 2.09 (H-4b), 2.05 (H-15a), 1.97 (H-7a), 1.54 (H-15b), 1.40 (H-7b); δ_C: 63.3 (C-20), 60.2 (C-12), 42.7 (C-4), 30.3 (C-7), 26.7(C-15), 23.8 (C-8)], three hypomethyl groups [δ_H: 2.90 (H-5), 2.52 (H-14), 2.29 (H-2); δ_C: 59.4 (C-2), 52.9 (C-14), 30.1 (C-5)], five methyl groups [δ_H: 2.10 (H-22), 1.54 (H-19), 1.13 (H-18), 1.01 (H-17), 1.00 (H-16); δ_C: 25.2 (C-16), 23.4 (C-17), 21.1 (C-18), 21.0 (C-22)], 20.6 (C-19)] and three quaternary carbons [δ_C: 51.8 (C-6), 49.7 (C-1), 40.4 (C-13)]. The ^{1}H-^{1}H COSY correlations of H-2/H-15/H-14; H-4/H-5/H-18; and H-7/H-8 along with HMBC correlations of H-2, H-4, H-15/C-3; H-18/C-4, C-5, C-6; H-16, H-17/C-1, C-2, C-6; H-7/C-5; H-19/C-10, C-12, C-13, C-14; H-20/C-8, C-9, C-10, C-21 and of H-22/C-21, elucidated the plannar structure of **1** as shown in Figure 1.

 doi:10.20944/preprints202409.2156.v1

The relative configuration of compound **1** was determined to be 2S*, 5R*, 6R*, 13S*, 14S* based on the NOESY correlations of H-16/H-14, H-2 and H-5/H-19. The absolute configuration of **1** was confirmed to be 2*S*, 5*R*, 6*R*, 13*S*, 14*S* by subsequent ECD calculations.

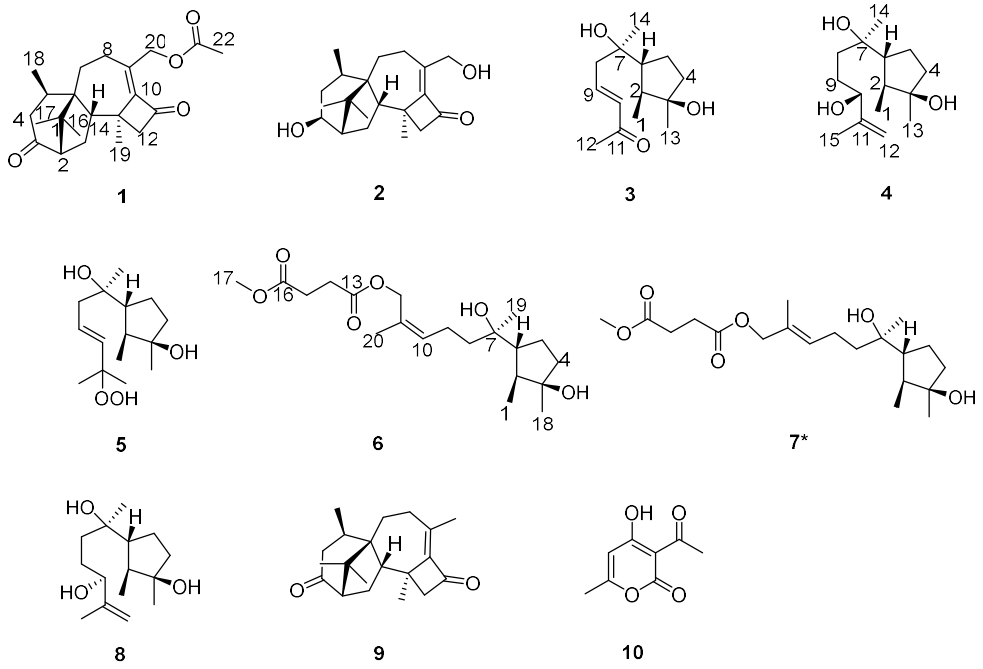

Figure 1. Chemical structures of compound **1**-**10**.

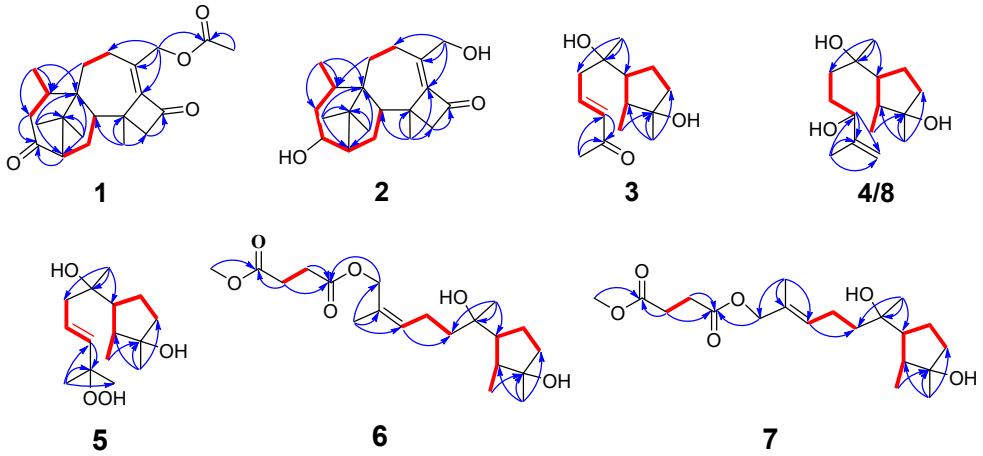

Figure 2. Key HMBC (bold lines) and ^{1}H–^{1}H COSY (arrows) correlations of compound **1–8**.

Compound **2** was purified as colorless oil, and its molecular formula was deduced to be $C_{20}H_{30}O_3$ by (+)-HRESIMS m/z 319.2268 $[M+H]^+$ (calcd. For $C_{20}H_{31}O_3^+$, 319.2268), implying six degrees of unsaturation. The IR spectrum of **2** showed absorption bands for hydroxyl (3439 cm^{-1}), methyl (2936 cm^{-1}) and carbonyl (1730 cm^{-1}). The ^{1}H-NMR, ^{13}C-NMR (Tables 1 and 2) and HSQC spectra indicate that compound **2** is a harziane diterpenes type compound like compound **1**, with the difference that the substituents of compound **2** at C-3 and C-20 are both hydroxyl groups. The entire structure was confirmed by the ^{1}H-^{1}H COSY correlations of H-14/H-15/H-2/H-3/H-4/H-5/H-18; H-7/H-8 and the HMBC correlations of H-7/C-5; H-12/C-11; H-16, H-17/C-1, C-2, C-6; H-18/C-4, C-5, C-6; H-19/C-10, C-12, C-13, C-14 as well as H-20/C-8, C-9, C-10. The relative configuration of compound **2** was assigned to be 2*S**, 3*S**, 5*R**, 6*R**, 13*S**, 14*S** by the NOESY correlation of H-15b/H-19, H-3; H-19/H-5.

 doi:10.20944/preprints202409.2156.v1

The experimental and calculated ECD spectra did match well, suggesting 2*S*, 3*S*, 5*R*, 6*R*, 13*S*, 14*S* was the correct absolute configuration (Figure 4).

Compound **3** was isolated as colorless oil, and its molecular formula was deduced to be C14H24O3 by (+)-HRESIMS m/z 263.1624 $[M+Na]^+$ (calcd. For $C_{14}H_{24}NaO_3^+$, 263.1618), implying three degrees of unsaturation. The FT-IR absorption band suggested the presence of hydroxy group (3436 cm^{-1}), methyl group (2958 cm^{-1}, 2926 cm^{-1} and 2850 cm^{-1}), olefinic group (1622 cm^{-1}) and carbonyl group (1666 cm^{-1}). The ^{1}H-NMR, ^{13}C-NMR (Tables 3 and 4) and HSQC spectra indicate the presence of one carbonyl signal [δ_C: 198.5 (C-11)], a group of conjugated olefin signals [δ_H: 6.88 (H-9), 6.13 (H-10); δ_C: 144.1 (C-9), 134.2 (C-10)], three aliphatic methylene signals [δ_H: 2.45 (H-8a), 2.36 (H-8b), 1.91 (H-5a), 1.72 (H-4a), 1.58 (H-4b, 5b); δ_C: 43.8 (C-8), 40.4 (C-4), 24.6 (C-5)], two hypomethyl signals [δ_H: 1.86 (H-6), 1.62 (H-2); δ_C: 54.9 (C-6), 44.6 (C-2)],two oxidized quaternary carbon signals [δ_C: 81.4 (C-3), 75.0 (C-7)] and four methyl signals [δ_H: 2.27 (H-12), 1.27 (H-13), 1.19 (H-14), 1.06 (H-1); δC: 27.2 (C-12), 26.2 (C-13), 25.9 (C-14) , 14.6 (C-1)]. The ^{1}H-^{1}H COSY correlations of H-1/H-2/H-6/H-5/H-4; H-8/H-9/H-10 as well as HMBC correlations of H-1/C-3, H-13/C-2, C-3, C-4; H-14/C-6, C-7, C-8; H-10/C-11 and of H-12/C-10, C-11 generated the planar structure of **3**. The configuration of the double bond at C-9 was assigned as *trans* by the NOESY correlations signal of H-8/H-10, and the large coupling constant between H-9 and H-10. The NOESY correlations of H-2/H-13 and H-1/H-6 indicates the relative configuration of C-2, C-3, C-6.

The absolute configuration of C-7 could not be determined by ECD. To solve this difficult stereoscopic problem, the NMR data of **3**a (2*S**, 3*R**, 6*R**, 7*R**) and **3**b (2*S**, 3*R**, 6*R**, 7*S**) were further calculated at the PCM/mPW1PW91/6–31+G (d, p) level using the GIAO method [**26]**. The calculated ^{13}C NMR chemical shifts of **3**a showed a better agreement with the experimental values of compound **3** with a higher correlation coefficient [R^2 for **3**a: 0.9958; R^2 for **3**b: 0.9956, Figure S 79]. In addition, DP4+ probability analysis [27] based on both ^{1}H and ^{13}C NMR data predicated **3**a as the correct relative structure with 96.49 % probability (Tables S 13). The experimental and calculated ECD spectra for 2*S*, 3*R*, 6*R*, 7*R* in MeOH did match well, indicating that 2*S*, 3*R*, 6*R*, 7*R* was the correct absolute configuration (Figure 4).

Compound **4** was isolated as colorless oil, its molecular formula was determined as $C_{15}H_{28}O_3$ by (+)-HRESIMS m/z 279.1940 $[M+Na]^+$ (calcd. For $C_{15}H_{28}NaO_3^+$, 279.1931), implying two degrees of unsaturation. The FT-IR absorption band indicate that compound **4** contains hydroxyl group (3424 cm^{-1}), methyl group (2962 and 2875 cm^{-1}), olefinic groups (1647 cm^{-1}). The planar structure of **4** was deduced to be the same as that of 11-cycloneren-3,7,10- triol [30] by comparison of its ^{1}H- and ^{13}C-NMR data (Tables 3 and 4) with those for **4**, which was supported by HMBC correlations of and ^{1}H-^{1}H COSY correlations (Figure 2).

The relative configurations of the cyclopentane in compound **4** were determined to be 2S*, 3R*, 6R* by the NOESY-related signals of H-1/H-6 as well as H-2/H-13. Since the amount of compound **4** was not sufficient for the Mosher's reaction, we determined its absolute configuration by calculating NMR and ECD. The relative configuration of the compound **4** was further determined to be 2*S**, 3*R**, 6*R**, 7*R**, 10*R** based on DP4+ probability (100% for 2*S**, 3*R**, 6*R**, 7*R**, 10*R**, Table S 26) analysis of ^{1}H-NMR and ^{13}C-NMR data. The absolute configuration of compound **4** was determined to be 2*S*, 3*R*, 6*R*, 7*R*, 10*R* based on the comparison of calculated and experimental ECD spectra (Figure 4).

Compound **5** was separated as colorless oil, with the molecular formula $C_{15}H_{28}O_4$ established by the (-)-HRESIMS data at m/z 271.1910 $[M-H]^-$ (calcd. For $C_{15}H_{27}O_4^-$ 271.1914), indicating two degrees of unsaturation. The FT-IR absorption band indicate that compound **5** contains hydroxyl group (3402 cm^{-1}) and methyl group (2966 and 2931 cm^{-1}). The NMR data of **5** (Tables 3 and 4) closely resembled those of 9-cycloneren-3, 7, 11-triol [30], with the main difference is that -OH at the C-10 is substituted with -OOH. This was demonstrated by the HRESIMS data and the HMBC correlations of H-10/H-11; H-12/H-10, H-11, H-15. Other HMBC and ^{1}H-^{1}H COSY correlations confirm the entire structure of the compound **5**. The trans relative configuration of C-9 and C-10 was established according to the large coupling constant of H-9 and H-10 and the NOESY correlations of H-10/H-8 (Figure 3). The relative configuration of **5** was determined to be 2*S**, 3*R**, 6*R** by NOESY cross-peaks of H-2/H-13 and of H-1/H-6.

Additionally, the relative configuration of C-7 was deduced as 7*R** by NMR calculations with the DP4+ probability of 100% (Table S 35). The absolute configuration of compound **5** was determined to be 2*S*, 3*R*, 6*R*, 7*R* by comparing the calculated ECD and experimental ECD spectra (Figure 4).

 doi:10.20944/preprints202409.2156.v1

Compound **6** was isolated as colorless oil, its molecular formula was deduced to be $C_{20}H_{34}O_6$ by (+)-HRESIMS m/z 393.2249 $[M+Na]^+$ (calcd. For $C_{20}H_{34}NaO_6^+$, 393.2248), with four degrees of unsaturation. The FT-IR absorption band suggested the presence of hydroxy group (3453 cm^{-1}), methyl group (2964 and 2937 cm^{-1}) and carbonyl group (1737 cm^{-1}). The ^{1}H-NMR, ^{13}C-NMR (Tables 1 and 2) and HSQC spectra indicate the presence of two carbonyl signal [δ_C: 172.9 (C-16), 172.4 (C-13)], a group of conjugated olefin signals [δ_H: 5.41 (H-10); δ_C: 131.2 (C-10), 129.9 (C-11)], six aliphatic methylene signals [δ_H: 2.64 (H-14, H-15), 2.19 (H-9a), 2.12 (H-9b), 1.85 (H-5a), 1.68 (H-4a), 1.56 (H-4b), 1.55 (H-5b), 1.49 (H-8); δ_C: 40.5 (C-4, C-8), 29.3 (C-15), 29.1 (C-14), 24.5 (C-5), 22.5 (C-9)], an oxidized methylene signal [δ_H: 4.66 (H-12a), 4.60 (H-12b); δ_C: 63.6 (C-12)], two hypomethyl signals [δ_H: 1.84 (H-6), 1.60 (H-2); δ_C: 54.6 (C-6), 44.4 (C-2)], two oxidized quaternary carbon signals [δ_C: 81.4 (C-3), 74.8 (C-7)] and four methyl signals [δ_H: 1.74 (H-20), 1.26 (H-18), 1.15 (H-19), 1.04 (H-1); δ_C: 26.2 (C-18), 25.0 (C-19), 21.6 (C-20), 14.7 (C-1)] and a methoxy signal [δ_H: 3.69 (H-17); 52.0 (C-17)].

The ^{1}H-^{1}H COSY correlations of H-1/H-2/H-6/H-5/H-4; H-8/H-9/H-10; H-14/H-15 as well as HMBC correlations of H-1/C-3; H-18/C-2, C-3, C-4; H-19/C-6, C-7, C-8; H-10/C-8; H-20/C-10, C-11, C-12; H-12/C-13; H-14/C-13; H-15/C-13, C-16 and of H-17/C-16 generated the primary structure of **6**. The configuration of the double bond at C-10 was assigned as cis by the NOESY correlations signal between H-9/H-12 as well as H-10/H-20. The correlations between H-2 and H-18, H-1 and H-6 suggests that the relative configurations of C-2, C-3 and C-6 are 2*S*, 3*R*, 6*R*.

The relative configuration of the C-7 is 7*R**, as shown by the theoretical NMR calculation using the GIAO's method combined with a DP4$^+$ probability analysis (Table S 44). The absolute configuration of **6** was confirmed by the similarity between the calculated ECD curve of 2*S*, 3*R*, 6*R*, 7*R*-**6** and its experimental ECD spectrum (Figure 4). Thus, the structure of **6** is as shown in Figure 1.

Compound **7** was obtained as colorless oil, The molecular formula $C_{20}H_{34}O_6$ was given by analysis of (+)-HRESIMS m/z 393.2252 $[M+Na]^+$ (calcd. For $C_{20}H_{34}NaO_6^+$, 393.2248), suggesting four degrees of unsaturation. The FT-IR absorption band shows the presence of hydroxyl (3456 cm^{-1}), methyl (2968 and 2936 cm^{-1}) and carbonyl (1738 cm^{-1}). Its ^{1}H- and ^{13}C-NMR (Tables 1 and 2) as well as HREIMS data closely resembled those of **7**, and ^{1}H-^{1}H COSY and HMBC correlations (Figure2) also suggested **8** has a similar planar structure to **7**. The difference between compound **8** and **7** is that the geometry of double bond at C-10 is trans which was inferred from the NOESY correlations of H-9/H-20 as well as H-10/H-12. The relative configuration of C-2, C-3, C-6 was determined to be 2*S*, 3*R*, 6*R* based on the correlation signals of H-2/H-18 as well as H-1/H-6 in the NOESY spectra (Figure 3).

The relative configuration of C-7 was determined by NMR calculations combined with DP4$^+$ probability analysis (100% for 2*S**, 3*R**, 6*R**, 7*R**, Table S 43). By contrast of the experimental and calculated ECD data, the absolute configuration was validated.

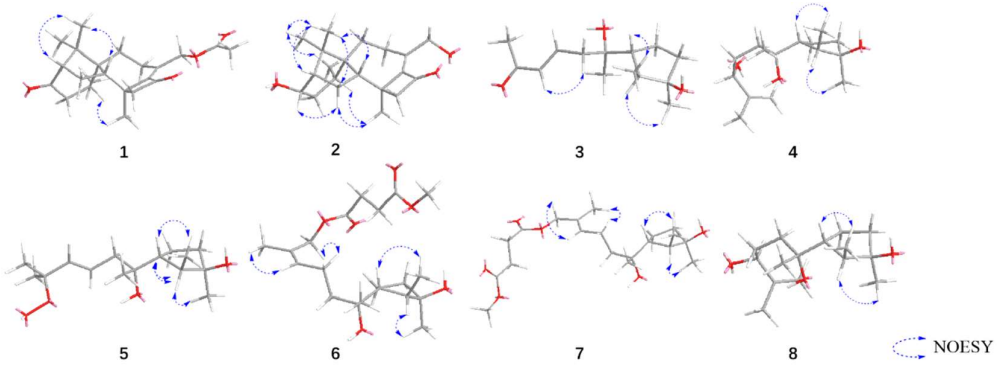

Figure 3. Key NOESY correlations of compound **1-8**.

 doi:10.20944/preprints202409.2156.v1

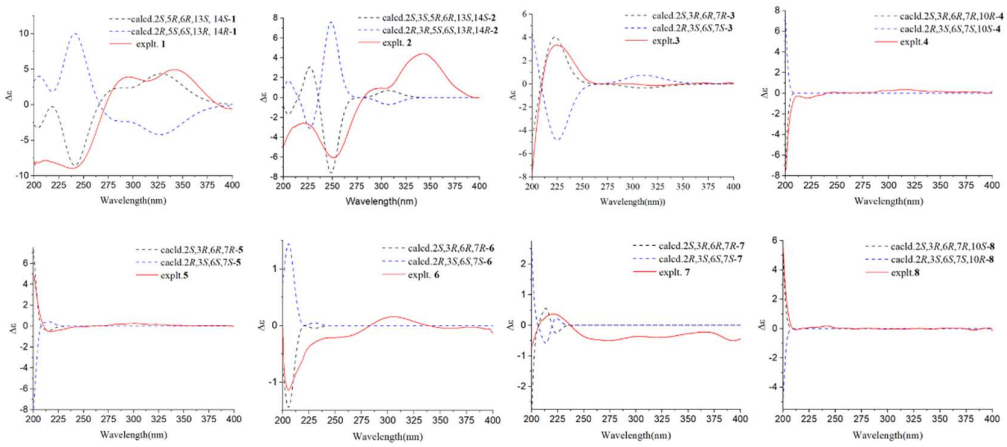

Figure 4. Calculated ECD spectra and experimental ECD curves of compound **1–8** in MeOH.

Compound **8** was obtained as colorless oil, its molecular formula was determined as $C_{15}H_{28}O_3$ by (+)-HRESIMS m/z 279.1941 $[M+Na]^+$ (calcd. For $C_{15}H_{28}NaO_3^+$, 279.1931), implying two degrees of unsaturation. The FT-IR absorption band indicate that compound **8** contains hydroxyl group (3408 cm^{-1}), methyl group (2960 and 2873cm^{-1}), olefinic groups (1647 cm^{-1}). The ^{1}H-NMR, ^{13}C-NMR (Tables 3 and 4) and HSQC spectra exhibited the presence of a group of olefinic signals [δ_H: 4.97 (H-12a), 4.86 (H-12b); δ_C: 147.7 (C-11), 111.0 (C-12)], four methylene groups [δ_H: 1.87 (H-5a), 1.71 (H-9a), 1.69 (H-4a), 1.61 (H-9b), 1.57 (H-8a, H-4b), 1.56 (H-5b), 1.50 (H-8b); δ_C: 40.5 (C-4), 35.8 (C-8), 29.1 (C-9), 24.5 (C-5)], two hypomethyl groups [δ_H: 1.87 (H-6), 1.59 (H-2); δ_C: 54.8 (C-6), 44.5 (C-2)], one oxidized hypomethyl group [δ_H: 4.09 (H-10); δ_C: 76.0 (C-10)], two oxidized quaternary carbon signals [δ_C: 81.4 (C-3), 74.8 (C-7)] and four methyl signals [δ_H: 1.72 (H-15), 1.26 (H-13) 1.16 (H-14), 1.04 (H-1); δ_C: 26.2 (C-13), 25.2 (C-14) , 18.2 (C-15), 14.6 (C-1)].

The ^{1}H-^{1}H COSY correlations of H-1/H-2/H-6/H-5/H-4; H-8/H-9/H-10 along with the HMBC correlations signals of H-1/C-3; H-13/C-2, C-3, C-4; H-14/C-6, C-7, C-8; H-10/C-11, C-12 and of H-15/C-10, C-11, C-12 demonstrated that compound **8** is 11-cycloneren-3, 7, 10-triol [24].According to previous research[33], the chirality of 11-cycloneren-3,7,10-triol at C-10 was undetermined, so the Mosher's method was used to determine its conformation. Compound **8** was esterified with (*S*)-MTPA-Cl and (*R*)-MTPA-Cl, respectively, to give Mosher ester derivatives. The $\Delta\delta_{S-R}$ of the ^{1}H-NMR data of each proton adjacent to C-10 in the (*S*)-MTPA ester and (*R*)-MTPA ester products were compared (Fig. 50), and the final absolute configuration of C-10 was determined to be 10*S*. The ECD of compound **8** was calculated, and the calculated ECD curves of 2*S*, 3*R*, 6*R*, 7*R*, 10*S*-**8** were found to be in good agreement with the experimental ECD curves, thus the absolute configuration of compound **8** was determined.

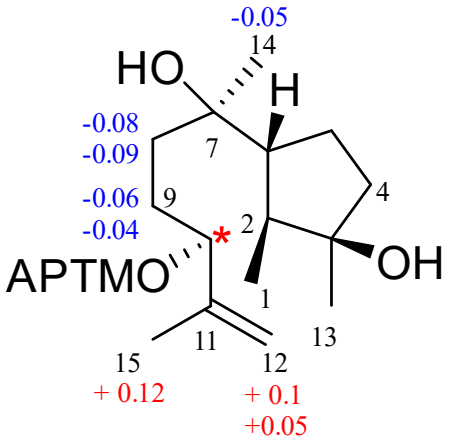

Figure 5. $\Delta\delta_{S-R}$ value (ppm) of MTPA ester of **8**.

 doi:10.20944/preprints202409.2156.v1

3.2. Fungicidal Activities of Compounds 1-10 In Vitro

Table 5. Activities of compound **1–10** against six kinds of pathogenic fungi[a].

compound	Fungicidal activities (%) at 50 μg/mL					
	A.S.	*F.G.*	*P.C.*	*S.S.*	*B.C.*	*R.S.*
1	52.2 ±2.3	56.5 ±4.2	45.7 ±1.5	**85.9 ±3.7**	44.7 ±5.1	19.3 ±0.6
2	39.1 ±3.4	17.4 ±1.1	21.7 ±32.6	**73.1 ±2.6**	26.3 ±2.5	46.5 ±4.5
3	56.5 ±4.2	34.8 ±2.0	42.8 ±2.5	**64.1 ±2.5**	**81.6 ±3.4**	28.1 ±3.4
4	47.8 ±1.7	23.9 ±1.6	32.6 ±2.4	**73.1 ±4.2**	42.1 ±2.6	15.1 ±2.3
5	45.8 ±2.4	26.1 ±2.5	23.9 ±2.2	**67.9 ±3.4**	39.5 ±4.3	19.3 ±3,6
6	30.4 ±3.5	**84.8 ±3.1**	26.1 ±1.1	**75.6 ±1.8**	47.4 ±2.1	17.4 ±2.1
7	34.8 ±1.9	15.2 ±1.4	35.0 ±3.1	51.3 ±2.3	34.2 ±1.4	14.0 ±1.5
8	30.4 ±2.4	28.3 ±2.6	37.0 ±2.2	53.8 ±4.1	26.3 ±2.6	51.2 ±3.9
9	12.5 ±1.2	23.1 ±3.4	9.4 ±0.6	**76.1 ±3.5**	46.2 ±3.6	59.4 ±4.3
10	56.3 ±3.6	38.5 ±3.2	28.1 ±1.8	**100.0 ±0.0**	**100.0 ±0.0**	**82.8 ±2.5**

[a] A.S.: Alternaria solani; F.G.: Fusarium graminearum; P.C.: Phytophthora capsici; S.S.: Sclerotinia sclerotiorum; B.C.: Botrytis cinerea; R.S.: Rhizoctonia solani.

We tested the fungicidal activity of compounds **1**-**10** against six crop pathogens at a concentration of 50 μg/mL. Fungicidal tests showed that compounds **1**-**10** all showed good inhibition of *S. sclerotiorum* at a concentration of 50 μg/mL. In addition, compound **3** and **10** showed significant inhibition against *B. cinerea* with inhibition rates of 81.6% and 100%, respectively.

3.3. Fungicidal Activities of Compound 10 In Vivo

In the in vivo activity test, compound **10** was effective against two pathogens, and it showed significant inhibitory activity against *B. cinerea*, with a control effect of 65.8%.

Table 6. Activities of compound **10** against *Botrytis cinerea* and *Sclerotinia sclerotiorum* in vivo.

Preventative efficiency (%)		
pathogenic fungi	*Botrytis cinerea*	*Sclerotinia sclerotiorum*
10	65.8 %	49.1 %
PC	88.6 %	100 %

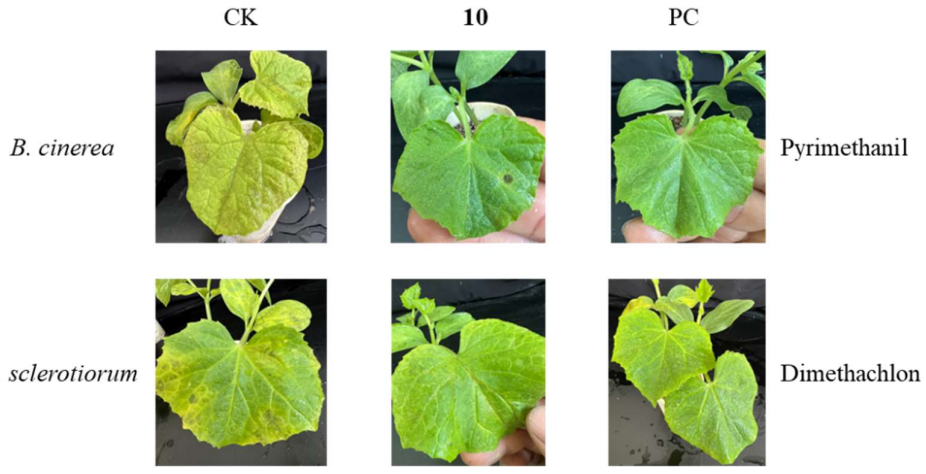

Figure 6. Activities of compound **10** against *B. cinerea* and *S. sclerotiorum* in vivo.

 doi:10.20944/preprints202409.2156.v1

4. Discussion

A variety of Trichoderma strains have been utilized worldwide as effective biocontrol agents, including *T. harzianum*, *T. hamatum*, *T. asperellum*, *T. atroviride*, *T. koningii*, and *T. viride* [31–35]. One of the mechanisms by which Trichoderma exerts biological control is through the production of secondary metabolites [36,37]. In the present study, we isolated and purified secondary metabolites extracted using ethyl acetate from *T. hamatum* and identified the structures of the previously undescribed compounds **1**-**7**, as well as the known compound **8**, utilizing HRESIMS, NMR, UV, IR, circular dichroism, and Mosher's method in conjunction with computational chemistry. Compounds **1**, **2**, and **9** are harziane diterpenes characterized by a unique 6-5-4-7 tetracyclic carbon skeleton; compounds **3**-**8** are cyclonerane sesquiterpenes, among which compound **5** represents the first -OOH-substituted cyclonerane sesquiterpene to be discovered, while compound **10** was identified as dehydroacetic acid.

Dehydroacetic acid (**10**) was first isolated from *Solandra nitida* in 1866 and has been utilized as a food preservative due to its efficacy in inhibiting the growth of molds, yeasts, and bacteria. Its derivatives have been investigated for the development of effective antimicrobial agents against various bacteria and fungi[38]; however, research on its antagonistic effects against agricultural pathogens remains relatively limited. In this study, the fungicidal activities of compounds **1**-**9** and dehydroacetic acid (**10**) against six agricultural pathogens were assessed. The results indicated that some of these compounds exhibited promising fungicidal activities against pathogenic fungi. Notably, dehydroacetic acid (**10**) significantly inhibited the growth of both *B. cinerea* and *R. solani*. Furthermore, in vivo examinations of the effects of dehydroacetic acid (**10**) on the control of *B. cinerea* and *S. sclerotiorum* suggested its potential for development as an agricultural antibiotic. Additionally, the substantial isolation of dehydroacetic acid may partially account for the antibiosis activity observed in *T. hamatum*.

This work not only enriched the active material base of *T. hamatum* but also advanced the application of its secondary metabolites in controlling agricultural pathogenic fungi, thereby providing a valuable reference for the development of fungal biocontrol strategies.

5. Patents

Chengdu University of Traditional Chinese Medicine has filed patents ZL202311414683.0 and ZL202311251991.6 concerning the *in vitro* antifungal activity of compounds **2** and **3**.

Supplementary Materials: The following supporting information can be downloaded at the website of this paper posted on Preprints.org, Figure S1-S9:HRESIMS, IR and NMR spectra for compound **1**; Figure S10-S18: HRESIMS, IR and NMR spectra for compound **2**; Figure S19-S27: HRESIMS, IR and NMR spectra for compound **3**; Figure S28-S36: HRESIMS, IR and NMR spectra for compound **4**; Figure S37-S45: HRESIMS, IR and NMR spectra for compound **5**; Figure S46-S54: HRESIMS, IR and NMR spectra for compound **6**; Figure S55-S63: HRESIMS, IR and NMR spectra for compound **7**; Figure S64-S72: HRESIMS, IR and NMR spectra for compound **8**; Figure S73-S110: Calculated NMR and calculated ECD supplementary figure for compound **1-8**; Table S1-S61: Calculated NMR and calculated ECD supplementary tables for compound **1-8**.

Author Contributions: Conceptualization, D. G, G.W. and Q.B.; methodology, Q.B. and Q.Z..; software, L.H.; validation, D.G., G.W. and L.C..; investigation, L.H., M.L., Y.H. and L.C.; resources, G.W.; data curation, L.H., M.L., Y.H. and L.C.; writing—original draft preparation, L.H.; writing—review and editing, D.G. and Y.G.; visualization, L.H.; supervision, G.W. and D.G.; funding acquisition, D.G. All authors have read and agreed to the published version of the manuscript.

Funding: This research was funded by Sichuan Science and Technology Program, grant number 2021YFN0134.

Data Availability Statement: The authors will make all raw data supporting the conclusions of this article available to any qualified researcher, without undue reservation.

Acknowledgments: On the auspicious occasion of her 95th birthday, this paper is dedicated to Professor Youyou Tu, the esteemed recipient of the 2015 Nobel Prize in Physiology or Medicine, in recognition of her groundbreaking discovery of Artemisinin, which has saved millions of lives worldwide.

Conflicts of Interest: The authors declare no conflicts of interest.

 doi:10.20944/preprints202409.2156.v1

References

1. Salazar, B.; Ortiz, A.; Keswani, C.; Minkina, T.; Mandzhieva, S.; Pratap, S. S.; Rekadwad, B.; Borriss, R.; Jain A.; Singh HB.; Sansinenea E. *Bacillus* spp. as Bio-factories for Antifungal Secondary Metabolites: Innovation Beyond Whole Organism Formulations. *Microb Ecol*, **2023**; *86*, 1-24. DOI: 10.1007/s00248-022-02044-2.
2. Syed Ab Rahman, S.F.; Singh, E.; Pieterse, C.M.J.; Schenk, P.M. Emerging microbial biocontrol strategies for plant pathogens. *Plant Sci*, **2018**, *267*, 102-111. DOI: 10.1016/j.plantsci.2017.11.012.
3. Saldaña-Mendoza, S.A.; Pacios-Michelena, S.; Palacios-Ponce, A.S.; Chávez-González, M.L.; Aguilar, C.N. *Trichoderma* as a biological control agent: mechanisms of action, benefits for crops and development of formulations. *World J Microbiol Biotechnol*, **2023**; *39*, 269. DOI: 10.1007/s11274-023-03695-0.
4. Li, Z.; Jennings, A. Worldwide Regulations of Standard Values of Pesticides for Human Health Risk Control: A Review. *Int J Environ Res Public Health*, **2017**, *14 (7)*, 826. DOI: 10.3390/ijerph14070826.
5. Harman, G.; Khadka, R.; Doni, F.; Uphoff, N. Benefits to Plant Health and Productivity from Enhancing Plant Microbial Symbionts. *Front Plant Sci*, **2021**, *11*, 610065. DOI: 10.3389/fpls.2020.610065.
6. Zhao, D.; Shen, D.; Fan, H.; Zhu, X.; Wang, Y.; Duan, Y.; Chen, L. Virulent and attenuated strains of *Trichoderma citrinoviride* mediated resistance and biological control mechanism in tomato. *Front Plant Sci*, **2023**, *14*, 1179605. DOI: 10.3389/fpls.2023.1179605.
7. Martinez, Y.; Ribera, J.; Schwarze F.W.M.R.; De France, K. Biotechnological development of Trichoderma-based formulations for biological control. *Appl Microbiol Biotechnol*, **2023**, *107 (18)*, 5595-5612. DOI: 10.1007/s00253-023-12687-x.
8. Tyśkiewicz, R.; Nowak, A.; Ozimek, E.; Jaroszuk-Ściseł, J. *Trichoderma*: The Current Status of Its Application in Agriculture for the Biocontrol of Fungal Phytopathogens and Stimulation of Plant Growth. *Int J Mol Sci*, **2022**, *23 (4)*, 2329. DOI: 10.3390/ijms23042329.
9. Yao, X.; Guo, H.; Zhang, K.; Zhao, M.; Ruan, J.; Chen, J. *Trichoderma* and its role in biological control of plant fungal and nematode disease. *Front Microbiol*, 2023, 14, 1160551. DOI: 10.3389/fmicb.2023.1160551.
10. Bolzonello, A.; Morbiato, L.; Tundo, S.; Sella, L.; Baccelli I.; Echeverrigaray S.; Musetti R.; De Zotti M.; Favaron F.; Peptide Analogs of a *Trichoderma* Peptaibol Effectively Control Downy Mildew in the Vineyard. *Plant Dis*, **2023**, *107 (9)*, 2643-2652. DOI: 10.1094/PDIS-09-22-2064-RE.
11. El-Hasan, A.; Walker, F.; Klaiber, I.; Schöne, J. P.; fannstiel, J.; Voegele, R.T. New Approaches to Manage Asian Soybean Rust (*Phakopsora pachyrhizi*) Using *Trichoderma* spp. or Their Antifungal Secondary Metabolites. *Metabolites*, **2022**, *12 (6)*, 507. DOI: https://doi.org/10.3390/metabo12060507.
12. Scharf, D.H.; Brakhage, A.A.; Mukherjee, P.K. Gliotoxin--bane or boon? *Environ Microbiol*, **2016**, *18 (4)*, 1096-1109. DOI: 10.1111/1462-2920.13080.
13. Lin, X.; Tang, Z.; Gan, Y.; Li, Z.; Luo, X.; Gao, C.; Zhao, L.; Chai, L.; Liu, Y. 18-Residue Peptaibols Produced by the Sponge-Derived *Trichoderma* sp. GXIMD 01001. *J Nat Prod*, **2023**, *86 (4)*, 994-1002. DOI: 10.1021/acs.jnatprod.3c00014.
14. Torres-Ortega, R.; Guillén-Alonso, H.; Alcalde-Vázquez, R.; Ramírez-Chávez, E.; Molina-Torres, J.; Winkler, R. In Vivo Low-Temperature Plasma Ionization Mass Spectrometry (LTP-MS) Reveals Regulation of 6-Pentyl-2H-Pyran-2-One (6-PP) as a Physiological Variable during Plant-Fungal Interaction. *Metabolites*, **2022**, *12 (12)*, 1231. DOI: 10.3390/metabo12121231.
15. Li, C.P.; Shi, Z.Z.; Fang, S.T.; Song, Y.P.; Ji, N.Y. Lipids and Terpenoids from the Deep-Sea Fungus *Trichoderma lixii* R22 and Their Antagonism against Two Wheat Pathogens. *Molecules*, **2023**, *28 (17)*, 6220. DOI: 10.3390/molecules28176220.
16. Hu, M.; Li, Q.L.; Yang, Y.B.; Liu, K.; Miao, C.P.; Zhao, L.X.; Ding, Z.T. Koninginins R-S from the endophytic fungus *Trichoderma koningiopsis*. *Nat Prod Res*, **2017**, *31 (7)*, 835-839. DOI: 10.1080/14786419.2016.1250086.
17. Ahluwalia, V.; Kumar, J.; Rana, V.S.; Sati, O.P.; Walia, S. Comparative evaluation of two *Trichoderma harzianum* strains for major secondary metabolite production and antifungal activity. *Nat Prod Res*, **2015**, *29 (10)*, 914-920. DOI: 10.1080/14786419.2014.958739.
18. Khan, R.A.A.; Najeeb, S.; Hussain, S.; Xie, B.; Li, Y. Bioactive Secondary Metabolites from *Trichoderma* spp. against Phytopathogenic Fungi. *Microorganisms*, **2020**, *8 (6)*, 817. DOI: 10.3390/microorganisms8060817.
19. Shi, Z.Z.; Liu, X.H.; Li, X.N.; Ji, N.Y. Antifungal and Antimicroalgal Trichothecene Sesquiterpenes from the Marine Algicolous Fungus *Trichoderma brevicompactum* A-DL-9-2. *J Agric Food Chem*, **2020**, *68 (52)*, 15440-15448. DOI: 10.1021/acs.jafc.0c05586.
20. Guo, Q.; Shi, L.; Wang, X.; Li, D.; Yin, Z.; Zhang, J.; Ding, G.; Chen, L. Structures and Biological Activities of Secondary Metabolites from the *Trichoderma* genus (Covering 2018-2022). *J Agric Food Chem*, **2023**, *71 (37)*, 13612-13632. DOI: 10.1021/acs.jafc.3c04540.
21. Ju, F.; Kuang, Q.X.; Li, Q.Z.; Huang, L.J.; Guo, W.X.; Gong, L.Q.; Dai, Y.F.; Wang, L.; Gu, Y.C.; Wang, D.; Deng, Y.; Guo, DL. Aureonitol Analogues and Orsellinic Acid Esters Isolated from *Chaetomium elatum* and Their Antineuroinflammatory Activity. *J Nat Prod*, **2021**, *84 (12)*, 3044-3054. DOI: 10.1021/acs.jnatprod.1c00783.
22. Kuang, Q.X.; Luo, Y.; Lei, L.R.; Guo, W.X.; Li, X.A.; Wang, Y.M.; Huo, X.Y.; Liu, M.D.; Zhang, Q.; Feng D.; Huang, L.J.; Wang, D.; Gu, Y.C.; Deng, Y.; Guo, D.L. Hydroanthraquinones from *Nigrospora sphaerica* and

Their Anti-inflammatory Activity Uncovered by Transcriptome Analysis. *J Nat Prod*, **2022**, *85 (6)*, 1474-1485. DOI: 10.1021/acs.jnatprod.1c01141.

23. Hoye, T. R.; Jeffrey, C. S.; Shao, F. Mosher ester analysis for the determination of absolute configuration of stereogenic (chiral) carbinol carbons. *Nat Protoc*, **2007**, *2 (10)*, 2451-2458. DOI: 10.1038/nprot.2007.354.
24. Zou, G.; Yang, W.; Chen, T.; Liu, Z.; Chen, Y.; Li, T.; Said, G.; Sun, B.; Wang, B.; She, Z. Griseofulvin enantiomers and bromine-containing griseofulvin derivatives with antifungal activity produced by the mangrove endophytic fungus Nigrospora sp. QQYB1. *Mar Life Sci Technol*, **2023**, 6 (1), 102-114. DOI: 10.1007/s42995-023-00210-0.
25. Goto, H.; Osawa, E. An efficient algorithm for searching low-energy conformers of cyclic and acyclic molecules. *J. Chem. Soc., Perkin Trans*, **1993**, *2*, 187−198. DOI: 10.1039/P29930000187.
26. Frisch, M.J.; Trucks, G.W.; Schlegel, H.B.; Scuseria, G.E.; Robb, M.A.; Cheeseman, J.R.; Scalmani, G.; Barone, V.; Petersson, G.A.; Nakatsuji, H.; Li, X.; *et al*. **2016**, Gaussian 16, Revision B.01, Gaussian, Inc., Wallingford CT.
27. Li, Y.H.; Mándi, A.; Li, H.L.; Li, X.M.; Li, X.; Meng, L.H.; Yang, S.Q.; Shi, X.S.; Kurtán, T.; Wang, B.G. Isolation and characterization of three pairs of verrucosidin epimers from the marine sediment-derived fungus Penicillium cyclopium and configuration revision of penicyrone A and related analogues. *Mar Life Sci Technol*, **2023**, 5 (2), 223-231. DOI: 10.1007/s42995-023-00173-2.
28. Grimblat, N.; Zanardi, M.M.; Sarotti, A.M. Beyond DP4: an Improved Probability for the Stereochemical Assignment of Isomeric Compounds using Quantum Chemical Calculations of NMR Shifts. *J Org Chem*, **2015**, *80 (24)*, 12526-12534. DOI: 10.1021/acs.joc.5b02396.
29. Bian, Q.; Zhao, R.Q.; Peng, X.J.; Gao, L.J.; Zhou, G.N.; Yu, S.J.; Zhao, W.G. Design, Synthesis, and Fungicidal Activities of Novel Piperidyl Thiazole Derivatives Containing Oxime Ether or Oxime Ester Moieties, *J Agric Food Chem*, **2021**, *69 (13)*, 3848-3858. DOI: 10.1021/acs.jafc.0c07581.
30. Song, Y.P.; Liu, X.H.; Shi, Z.Z.; Miao, F.P.; Fang, S.T.; Ji, N.Y. Bisabolane, cyclonerane, and harziane derivatives from the marine-alga-endophytic fungus *Trichoderma asperellum* cf44-2. *Phytochemistry*, **2018**, *152*, 45-52. DOI: 10.1016/j.phytochem.2018.04.017.
31. González-Menéndez, V.; Pérez-Bonilla, M.; Pérez-Victoria, I.; *et al*. Multicomponent Analysis of the Differential Induction of Secondary Metabolite Profiles in Fungal Endophytes. *Molecules*, **2016**, 21 (2), 234. DOI: 10.3390/molecules21020234.
32. Guo, R.; Li, G.; Zhang, Z.; *et al*. Structures and Biological Activities of Secondary Metabolites from *Trichoderma harzianum*. *Mar Drugs*, **2022**, *20 (11)*, 701. DOI: 10.3390/md20110701.
33. Guzmán-Guzmán, P.; Kumar, A.; de Los Santos-Villalobos, S.; *et al*. *Trichoderma* Species: Our Best Fungal Allies in the Biocontrol of Plant Diseases-A Review. *Plants (Basel)*, **2023**, *12 (3)*, 432. DOI: 10.3390/plants12030432.
34. Carrero-Carrón, I.; Trapero-Casas, J.L.; Olivares-García, C.; *et al*. *Trichoderma asperellum* is effective for biocontrol of Verticillium wilt in olive caused by the defoliating pathotype of *Verticillium dahliae*. *Crop Prot*, **2016**, *88*, 45-52. DOI: 10.1016/j.cropro.2016.05.009.
35. Guo R, Ji.S.; Wang, Z.; *et al*. *Trichoderma asperellum* xylanases promote growth and induce resistance in poplar. *Microbiol Res*, **2021**, *248*, 126767. DOI: 10.1016/j.micres.2021.126767.
36. Bhardwaj, N.; Kumar, J. Characterization of volatile secondary metabolites from *Trichoderma asperellum*. *JANS*, **2017**, *9*, 954-959. DOI: 10.31018/jans.v9i2.1303.
37. Alfiky, A.; Weisskopf, L. Deciphering *Trichoderma*-Plant-Pathogen Interactions for Better Development of Biocontrol Applications. *J. Fungi*, **2021**, *7 (1)*, 61. DOI: 10.3390/jof7010061.
38. Grover, A.; Kumar, A.; Tittal, R.K.; *et al*. Dehydroacetic acid a privileged medicinal scaffold: A concise review. *Arch pharm*, **2023**, *357 (2)*, e2300512. DOI: 10.1002/ardp.202300512.